Eur. Phys. J. A **6**, 203–210 (1999)

THE EUROPEAN PHYSICAL JOURNAL A

Nucleon form factors in a relativistic quark model*

Y.B. Dong[a], A. Faessler, K. Shimizu[b]

Institüt für Theoretische Physik, Universität of Tübingen, 72076 Tübingen, Germany

Received: 10 March 1999 / Revised version: 14 June 1999
Communicated by F. Lenz

Abstract. Electromagnetic form factors of protons and neutrons are investigated based on a relativistic quark model with the inclusion of a pion cloud. Pseudo-scalar π-quark interaction is employed to study the coupling between the nucleon and the π. The results show the important role of the pion cloud for the neutron charge form factor. Moreover, our numerical analysis indicates a difference between the relativistic and the nonrelativistic treatments.

PACS. 12.39.Jh Nonrelativistic quark model – 12.39.Ki Relativistic quark model – 12.39.Pn Potential models – 12.40.Vv Vector-meson dominance – 12.40.Yx Hadron mass models and calculations – 13.40.Em Electric and magnetic moments – 13.40.Gp Electromagnetic form factors – 13.40.Hq Electromagnetic decays

1 Introduction

For a long time constituent quark models have been employed to study the mass spectrum, form factors and transition properties of the nucleon and its resonances [1-2]. Usually constituent quark models are based on a nonrelativistic approach with relativistic corrections up to second order v^2/c^2. Relativistic effects on transition operators, on configuration mixing of the baryon wave functions caused by QCD inspired hyperfine interaction, and on form factors of the nucleon, such as axial-vector form factors, have already been studied in constituent quark models. The results indicate the necessity to extend the model to a fully relativistic one [3-4]. In the nonrelativistic constituent quark model, the effective degrees of freedom are massive quarks moving in a self-consistent potential [5] with relativistic corrections. Other degrees of freedom are not considered in its original version. Recently, data about the baryon spectrum and certain electromagnetic properties of the nucleons and its resonances, for example the spin structure of the nucleon, the helicity amplitudes to the $\Delta(1232)$ resonance and the mean square of the neutron charge radius r^2_{En}, show that although the constituent quark models are successful in explaining many static properties of the nucleons and the resonances, such as the magnetic moments of the proton and the neutron, and even the nucleon-nucleon interaction [6], other degrees of freedom like Goldstone bosons or gluons inside the nucleon must be included explicitly in order to explain some specify data. In fact, the experiments for the nucleon spin structure functions both in the deep inelastic scattering and in the low energy regions have already proven that hadrons are more complex systems with additional degrees of freedom which are not included in the conventional constituent quark models. Theoretically, the chiral quark model [7] and cloudy bag model [8-9] with Goldstone bosons degrees of freedom explicitly in the nucleon wave function are successful to understand the nucleon spin structure and the pion nucleon interaction. It is expected that more precise experiments to test also other degrees of freedom of the nucleon will be published soon [10]. Even at low-momentum transfer, such as in the real photon limit of the electromagnetic interaction between the nucleon and the photon, theoretical studies have shown the remarkable influence of the pion cloud on the form factors of the proton and the neutron and on the helicity amplitudes for the electromagnetic transitions between the nucleon, the $\Delta(1232)$ resonance and the Roper $N^*(1440)$ resonance [9,11-12].

To understand better the nonzero charge form factors and the nonzero mean square charge radius of the neutron $r^2_{En} = -0.119 fm^2$ [13] is still an interesting aim, even though the contribution from the neutron Pauli form factor F_2 to the neutron mean square charge radius (the contribution from the Foldy term to the square of the neutron charge radius is $3F_2^N(0)/2M_N^2 = -0.126 fm^2$) almost coincides with the measured data. A recent analysis by Isgur [14] indicates that this contribution by the Foldy term does not really explain the neutron charge radius

* Supported by the Alexander von Humboldt Foundation and the DAAD

[a] On leave from Institute of High Energy Physics, Academia Sinica, Beijing 100039, P. R. China

[b] On leave from Department of Physics, Sophia University, Tokyo, Japan

and its charge distribution, because in the leading order of the relativistic approximation to the constituent quark model in which the Foldy term first appears, it is canceled exactly by a contribution to the Dirac form factor F_1 of the neutron [14]. In this sense, the mean square of the neutron charge radius r^2_{En} can still be interpreted as coming from the charge distribution of the neutron system. Consequently, the study of the neutron charge distribution is nontrivial and it reveals vital information on the structure of the nucleon [14]. In this paper, the relativistic quark model with the pion degrees of freedom is employed to calculate the electromagnetic form factors of the proton and the neutron, in particular the charged form factor and mean square charged radius of the neutron. The pseudoscalar interaction between the quark and pion is used in order to describe the three quark core and the pion cloud. We also study the dependence of the physical observables on the parameters such as the effective quark mass in order to compare with the results of the nonrelativistic constituent quark model.

2 Relativistic quark model

In the followings, we will briefly outline our relativistic quark model which is similar to the cloudy bag model [7-9]. The cloudy bag model, which explicitly includes pions, has been investigated for a long time by Theberge, Thomas and Miller [8], by Kälbermann and Eisenberg and by Bermuth, Drechsel, Tialor and Seaborn [9]. In our model, each quark inside a nucleon is moving independently in a mean field of a scalar-vector type harmonic oscillator confinement potential

$$V_{Conf} = \frac{a_c}{2}(1+\gamma_0)r^2 = V_s(r) + V_v(r). \quad (1)$$

Here a_c is the strength of the confinement and $V_{s,v}$ stand for the scalar and vector confinement potentials, respectively. This form of the confinement potential allows analytical solutions of the Dirac equation. QCD yields asymptotically a linear confinement. But previous work [6] has shown that as long as the baryons have about the same radius, their properties do not depend on the radial dependence of the confinement potential, if the confinement strength is adjusted to reproduce the root mean charge radius. The single quark wave function can be obtained by solving the following Dirac equation

$$(\boldsymbol{\alpha}\cdot\boldsymbol{p} + \gamma_0(V_{conf}(r) + m_q) - E_{nl}) \mid \psi_{nl}(\boldsymbol{r}) >= 0, \quad (2)$$

where m_q is the quark mass, n,l =0,1,2,... are radial and orbital angular momentum quantum numbers, respectively. The relations of the energy eigenvalue E_{nl} of the above Dirac equation (2) to the confinement strength a_c and to the harmonic oscillator constant α_{nl} are

$$a_c = \frac{(E_{nl}-m_q)^2(E_{nl}+m_q)}{4(2n+l+3/2)^2},$$
$$\alpha_{nl} = \sqrt{a_c(E_{nl}+m_q)} = \frac{1}{b^2_{nl}}, \quad (3)$$

where b_{nl} is the harmonic oscillator length. The single quark ground state (n,l=0) wave function is

$$\psi_{0s}(\boldsymbol{r}) = \left(\frac{\alpha_{0s}}{\pi}\right)^{3/4}\left(1+\frac{E_{0s}-m_q}{2(E_{0s}+m_q)}\right)^{-1/2} \times \begin{pmatrix} i \\ -\frac{\alpha_{0s}}{E_{0s}+m_q}\boldsymbol{\sigma}\cdot\boldsymbol{r}\end{pmatrix}\exp\left(-\frac{\alpha_{0s}\boldsymbol{r}^{\,2}}{2}\right). \quad (4)$$

An analytical expression for the single quark wave function of the Dirac equation(2) is the advantage of the special scalar-vector harmonic oscillator confinement in (1) [15]. Unlike for the nonrelativistic harmonic oscillator model, here the harmonic oscillator constant depends on the radial and the orbital quantum numbers n, l [15]. However, the eigen-functions of the Dirac equation (2) are orthonormal to each other for the different quantum numbers n and l. In our numerical calculations, we have fixed the single quark ground state eigenvalue of (2) $E_{0s} = 540MeV$. Then, the strength of the confinement a_c and the harmonic oscillator constant α_{0s} are functions of the quark mass and can be determined by (3). This equation implies that an increase of the quark mass enhances the harmonic oscillator length $b_{0s} = 1/\sqrt{\alpha_{0s}}$ for the single quark wave function and decreases the harmonic oscillator constant α_{0s} and the strength of the confinement a_c accordingly. These results also indicate that a decrease of the confinement strength can be compensated by an increase of the quark mass m_q if the energy eigenvalue E_{0s} of a single quark is unchanged. As a result of these changes, the nucleon gets a larger radius and the harmonic oscillator length is enlarged simultaneously. It should be mentioned that in the constituent quark model, the harmonic oscillator length and the effective quark mass are usually selected to be about 0.5fm and 313MeV, respectively. If we choose these two parameters for the Dirac equation in our relativistic quark model, then for the eigenvalue of the single quark of (2) we get a value $E_{0S} = 752MeV$ from (3).

We first treat the nucleon as a three-quark bound state. Then, the Hamiltonian of the system is the sum of three single quark Hamiltonians. As a result, the equation for the total system is similar to the Breit equation [16], which has the correct Dirac limit. The proton and the neutron wave functions are in the simplest approach: the product of the three individual single quark wave functions. However, the center of mass motion should be removed. For this purpose, we use the Peierls-Yoccoz method which was also employed by Tegen, Brockmann and Weise (see [15]). In this approach one projects on a good total momentum $\boldsymbol{P}$. It should be mentioned that there are several other approximate treatments to remove the center of mass motion in a relativistic approach [17]. For example the simplified Peierls-Thouless method which recently was employed by Lu, Thomas and Williams [18]. Both methods of [15, 18] can only approximately remove the center of mass motion in a relativistic many-body system [17]. A detailed analysis of the different approaches for the removal of the center of mass motion is given in our recent work [19]. After removing the center of mass motion of the three quark wave

function, we can express it as

$$\Psi^B_{\boldsymbol{P}}(\boldsymbol{r}_1,\boldsymbol{r}_2,\boldsymbol{r}_3) = \frac{N_B(\boldsymbol{P})}{(2\pi)^9} \times \int d^3p_1 d^3p_2 d^3p_3 e^{i\boldsymbol{p}_1\cdot\boldsymbol{r}_1+i\boldsymbol{p}_2\cdot\boldsymbol{r}_2+i\boldsymbol{p}_3\cdot\boldsymbol{r}_3} \times \Psi^B_{\boldsymbol{P}}(\boldsymbol{p}_1,\boldsymbol{p}_2,\boldsymbol{p}_3), \quad (5)$$

where $\boldsymbol{P}=\boldsymbol{p}_1+\boldsymbol{p}_2+\boldsymbol{p}_3$ is the total three momentum of the three-quark core and $N_B(\boldsymbol{P})$ is a normalization constant for the baryon B. In a relativistic approach the intrinsic three-body wave function in [15] and in (5) and the normalization constant N_B depend on the total momentum $\boldsymbol{P}$ and on the method to remove the center of mass motion within a relativistic quark model with a self-consistent potential. If one projects always on the total momentum zero and then boosts the wave function to the center of mass momentum $\boldsymbol{P}$ with the above method, one obtains a slightly different intrinsic wave function than when one projects immediately on the total momentum $\boldsymbol{P}$. Thus one gets different values for the root mean square radius and the magnetic moment for the nucleon in the two cases. In the latter case (direct projection on $\boldsymbol{P}$) the limits of the total momentum $\boldsymbol{P}$ to zero for the form factors and other observables yield different values than, if one projects immediately to $\boldsymbol{P}=0$. This differences reflect the fact that one is not able to remove the center of mass motion in a completely covariant way from a relativistic many body wave function involving a common potential.

In (5), $\Psi^B_{\boldsymbol{P}}(\boldsymbol{p}_1,\boldsymbol{p}_2,\boldsymbol{p}_3)$ is the three-quark core wave function inside the baryon B in momentum space. For the nucleon, all three quarks are in the ground state. It is

$$\Psi^N_{\boldsymbol{P}}(\boldsymbol{p}_1,\boldsymbol{p}_2,\boldsymbol{p}_3;\alpha_{0s}) = (2\pi)^3\delta^3(\boldsymbol{p}_1+\boldsymbol{p}_2+\boldsymbol{p}_3-\boldsymbol{P}) \times \psi_{0s}(\boldsymbol{p}_1)\psi_{0s}(\boldsymbol{p}_2)\psi_{0s}(\boldsymbol{p}_3), \quad (6)$$

where $\psi_{0s}(\boldsymbol{p}_i)$ is the Fourier transformation of the single particle ground state wave function in coordinate space $\psi_{0s}(\boldsymbol{p}) = \int \psi_{0s}(\boldsymbol{r})e^{-i\boldsymbol{p}\cdot\boldsymbol{r}}d^3r$. The flavor part of the nucleon wave function is the same as the one in the nonrelativistic case. In (6) we project the nucleon wave function to the total momentum $\boldsymbol{P}$. It should be stressed that the total energy of the nucleon is $3E_q^{0s} = 1620MeV$ before the center of mass motion is removed. It is thus much larger than the averaged nucleon and $\Delta(1232)$ mass $M = (M_N + M_\Delta) = 1085MeV$. However, if one removes the center of mass motion, the total energy in the center of mass frame of the nucleon $\boldsymbol{P}=0$ will decreases to $2E_{0s}$ (see [15]). The wave function shown in (5) or (6) is the intrinsic wave function of the nucleon. In our approach (as in any relativistic approach with the common potential) the center of mass motion of the nucleon is only approximately removed in the wave function (5) or (6) due to the small component of the Dirac spinor in (4).

It is obvious that the kinetic energy and the contribution from the confinement decrease with increasing single quark effective mass. In the limit of $m_q = 0$, the nucleon mass mainly originates from the kinetic energy and the confinement potential. When the quark mass is enlarged to around $m_q \simeq M_N/3 = 313MeV$, the kinetic energy and the confinement potential decrease, however, they still contribute around 30% to the nucleon rest mass. This conclusion differs from the nonrelativistic constituent quark model, because in it the effective constituent quark mass is $m_q \sim M_N/3$, the nucleon mass is mainly the sum of the three effective constituent quark masses and the nucleon is only weakly bound. This is due to the fact that in a relativistic approach the scalar quantity (for example the mass term in the relativistic representation) is always smaller than the one in the nonrelativistic case. That is because of the small component in the relativistic Dirac wave function. Moreover, if we select the same parameters for the effective quark mass and the harmonic oscillator length b as in the nonrelativistic constituent quark model, namely $m_q = 313$MeV and $b = 0.5$fm, then in our model the single quark energy will be enlarged to 752MeV and the total nucleon mass at the rest will be 1500MeV even after the center of mass motion is removed. This feature is largely the cause of the discrepancy between the relativistic and the nonrelativistic approaches.

3 Inclusion of the meson cloud

To consider the effects of the pion cloud on the electromagnetic form factors of the proton and the neutron, we start from the following quark and pion Lagrangian

$$\mathcal{L}_{total} = \mathcal{L}_q + \mathcal{L}_\pi, \quad (7)$$

where

$$\mathcal{L}_q = \frac{i}{2}\bar\psi(\boldsymbol{r})\gamma^\mu \overleftrightarrow{\partial}_\mu \psi(\boldsymbol{r}) - \bar\psi(\boldsymbol{r})[V_{conf}(r)+m_q]\psi(\boldsymbol{r}) \quad (8)$$

$$\mathcal{L}_\pi = \frac{1}{2}(\partial_\mu\phi_\pi(\boldsymbol{r}))^2 - \frac{1}{2}m_\pi^2\phi_\pi^2(\boldsymbol{r}),$$

where ϕ_π is pion field. After a chiral transformation of the quark field $\psi(\boldsymbol{r})$

$$\psi(\boldsymbol{r}) \to \psi(\boldsymbol{r}) - i\gamma_5\frac{\boldsymbol{\tau}\cdot\boldsymbol{\pi}}{2f_\pi}\psi(\boldsymbol{r}), \quad (9)$$

we get the pseudo-scalar pion-quark interaction

$$\mathcal{L}_{qq\pi} = \frac{i}{f_\pi}\bar\psi(\boldsymbol{r})\gamma^5(V_s(r)+m_q)\boldsymbol{\tau}\psi(\boldsymbol{r})\cdot\boldsymbol{\phi}_\pi(\boldsymbol{r}), \quad (10)$$

where $f_\pi = 93$MeV is the pion decay constant, and

$$\phi_\pi(\boldsymbol{r}) = \int \frac{d^3k}{[2\omega_k(2\pi)^3]^{1/2}}[a(\boldsymbol{k})e^{i\boldsymbol{k}\cdot\boldsymbol{r}} + a^+(\boldsymbol{k})e^{-i\boldsymbol{k}\cdot\boldsymbol{r}}]. \quad (11)$$

In (11) ω_k and $\boldsymbol{k}$ are the energy and the three momentum of the pion, respectively. In our previous calculations for the properties of the nucleon and the $\Delta(1232)$ resonance [12], it has been proven that this pion quark interaction $\mathcal{L}_{qq\pi}$ can give a good description for the empirical nucleon pion coupling constant. In (8), we explicitly include the pion and quark masses in our Lagrangian.

The physical pion mass $m_\pi = 140MeV$ is small compared to the hadronic scale of around 1GeV. The pion mass has the important relation to the current quark mass [20-21] $m_\pi^2 f_\pi^2 = -\frac{1}{2}(m_u + m_d) < q\bar{q} >$ (where $< q\bar{q} >=< u\bar{u} > + < d\bar{d} >$ is the vacuum expectation value of quark pairs: quark condensete [20-21]). Moreover, the pion mass $m_\pi = 140$MeV relates to the four-divergence of the total axial current $A^\mu(x)$ due to quarks and pions as

$$\partial_\mu A^\mu(x) = -f_\pi m_\pi^2 \phi_\pi(x), \tag{12}$$

Thus, the four-divergence of the total axial-vector current $A^\mu(x)$ is not conserved. This is the PCAC relation [20-21]. In soft pion limit $m_\pi \to 0$, the four-divergence implies a conserved axial current.

To include the effects of the pion cloud in the electromagnetic interaction of the nucleon, we perform a minimal substitution in (8). The additional electromagnetic current describes the photon-pion coupling is

$$j^\mu_{\pi\gamma} = ie[\phi^+_{\pi^+}(\boldsymbol{r})\partial^\mu\phi_{\pi^+}(\boldsymbol{r}) - \phi_{\pi^+}(\boldsymbol{r})\partial^\mu\phi^+_{\pi^+}(\boldsymbol{r})], \tag{13}$$

where $\phi_{\pi^+} = \frac{1}{\sqrt{2}}[\phi_1(\pi)+i\phi_2(\pi)]$, either destroys a negative or creates a positive charged pion. Thus, the electromagnetic field interacts with the total current:

$$J^\mu = j^\mu_{q\gamma} + j^\mu_{\pi\gamma}. \tag{14}$$

In (14) $j^\mu_{q\gamma}$ is usual "impulse" current, which leads to the quark-photon coupling

$$j^\mu_{q\gamma} = \sum_i e_i \Psi^+\gamma_0(i)\gamma^\mu(i)\exp(i\boldsymbol{q}\cdot\boldsymbol{r}_i)\Psi, \tag{15}$$

where $\boldsymbol{q}$ is the photon three momentum. After inclusion of the pion cloud, the total wave functions for the proton and the neutron can be re-written in an extend Fock space

$$\mid \tilde{B} >= Z_2^B[\mid \Psi^B > + \sum_{B'=N,\Delta} C^{BB'} \mid (\Psi^{B'}\pi)_B >], \tag{16}$$

where Z_2^B is a renormalization constant for the baryon resonance B, and B' is restricted in this work to be only N and $\Delta(1232)$ resonances for the intermediate states like in the cloudy bag model [8-9]. For the intermediate state, we take pion as a Goldstone boson and antisymmetrize the wave functions of the baryons (, this means of the nucleons and Δ resonances, respectively). One can easily find from the above expression for the nucleon wave function (16) that the charge distribution inside a neutron differs from the one in the three-quark core, because in the second term of (16), the charged pions also contribute to the neutron wave function. As a result the mean square of the neutron charge radius is nonzero. The probability of the pion-baryon admixture to the wave function of the nucleon $\mid C^{BB'} \mid^2$ can be calculated simply by using perturbation theory as shown in [22-23]. Moreover, the detailed calculation for the meson cloud and the renormalization constant in (16) in the extended Fock space with one pion in the cloud is described in [8,22-23]. In our calculation, we simply use 938MeV and 1232MeV for the masses of the nucleon and the Δ resonance in the baryon-pion sector $\mid (\Psi^{B'}\pi)_B >$. In this way, the probability of the component of $\mid \Delta\pi >$ is suppressed compared to that of $\mid N\pi >$ because of the energy denominator. Since we focus on the electromagnetic form factor of the nucleon, we do not consider any contribution from one-gluon exchange interaction and do not specify the splitting between the $\Delta(1232)$ and nucleon in this work. In the nonrelativistic constituent quark model, the mass splitting between the nucleon and the Δ comes mainly from the spin dependent part of the one-gluon and one pion exchanges. The discussion for the mass splitting between the nucleon and Δ due to the pion cloud is given in [24] by cloudy bag model.

Figures 1-4 display our calculated results for the proton and the neutron electric and magnetic form factors in the Breit frame when the effective quark mass is chosen $m_q = 0$. In Figs. 1-4, the data are quoted from [25-31]. In Fig. 5, we show the diagrams which we include in our calculation for the quark core and the pion cloud. Figure 5a is the impulse coupling between the quark and the photon without a pion cloud. Figure 5b stands for the interference between the parts of the wave function of the nucleon describing the pion cloud and the three quarks. Figure 5c represents the pion-photon coupling. Figures 5b and 5c contain both the pion exchange between two different quarks and the pion cloud of a single quark. In Table 1, we list our calculated results for the mean square radii of the proton and the neutron charge distributions and the magnetic moments of the proton and the neutron, respectively. In the table, three sets of results for different quark masses $m_q = 0, 150$MeV and 300MeV are listed. We also display separately each contribution of the three diagrams in Fig. 5 in order to see their effects more explicitly.

4 Conclusions

The results presented here are based on a relativistic constituent quark model with the pion cloud included explicitly. In our calculation, the eigenvalue for single quark Dirac (2) is fixed to be $E_{0s} = 540$MeV in order to get roughly the correct experimental averaged nucleon and $\Delta(1232)$ mass. The relativistic calculation of this work are different from the nonrelativistic approach. The difference originates from the adjusted effective parameters, such as the effective quark mass and the harmonic oscillator length b_{0s}. In the nonrelativistic approach, these two parameters are favored to be about $M_N/3 = 313MeV$ and 0.5fm. However, these values of the parameters are not applicable in our relativistic approach, because the corresponding eigenvalue for single quark is 752MeV and the predicted nucleon mass in the center of nucleon mass frame is more than 1700MeV. On the other hand, if we fix the eigenvalue of the Dirac (2) for the single quark to be $E_{0s} = 540MeV$ and select the effective quark mass $m_q = 350MeV$, the harmonic oscillator length for the single wave function derived from this value (3) is about 0.83fm. This value is not optimal to describe the nucleon

Table 1. Physical observables for the proton and for the neutron calculated in our model after re-normalization ($E_{0s} = 540MeV$). The quark masses m_q, mean square radii $< r^2_{Ep,En} >$, root mean square radius $\sqrt{< r^2_{Ep} >}$ and magnetic moments $\mu_{p,n}$ are in units of MeV, fm^2, fm and nuclear magnetons μ_N, respectively. The observables are given for three different quark masses m_q. The contributions of the diagrams in Figs. 5a (impulse approximation), 5b (interference between 3q and pion) and 5c (pion contribution) are shown separately

	m_q [MeV]	$< r^2_{Ep} >$ $[fm^2]$	$\sqrt{< r^2_{Ep} >}$ $[fm]$	$< r^2_{En} >$ $[fm^2]$	μ_p $[e\hbar/(2M_Nc)]$	μ_n $[e\hbar/(2M_Nc)]$
Fig. 5a	0	0.469		0	2.044	-1.362
Fig. 5b		0.0687		0.0412	0.101	-0.0773
Fig. 5c		0.137		-0.137	0.346	-0.346
Total		0.685	0.827	-0.0958	2.491	-1.785
Fig. 5a	150	0.441		0	1.767	-1.178
Fig. 5b		0.0822		0.0403	0.129	-0.0689
Fig. 5c		0.128		-0.128	0.376	-0.375
Total		0.651	0.807	-0.0877	2.272	-1.622
Fig. 5a	300	0.522		0	1.568	-1.045
Fig. 5b		0.0929		0.0518	0.0998	-0.0669
Fig. 5c		0.139		-0.139	0.387	-0.387
Total		0.754	0.868	-0.0872	2.055	-1.499
Expt. Data			0.847 ± 0.008[30]	-0.113 ± 0.005[13]	2.7928[35]	-1.913[35]

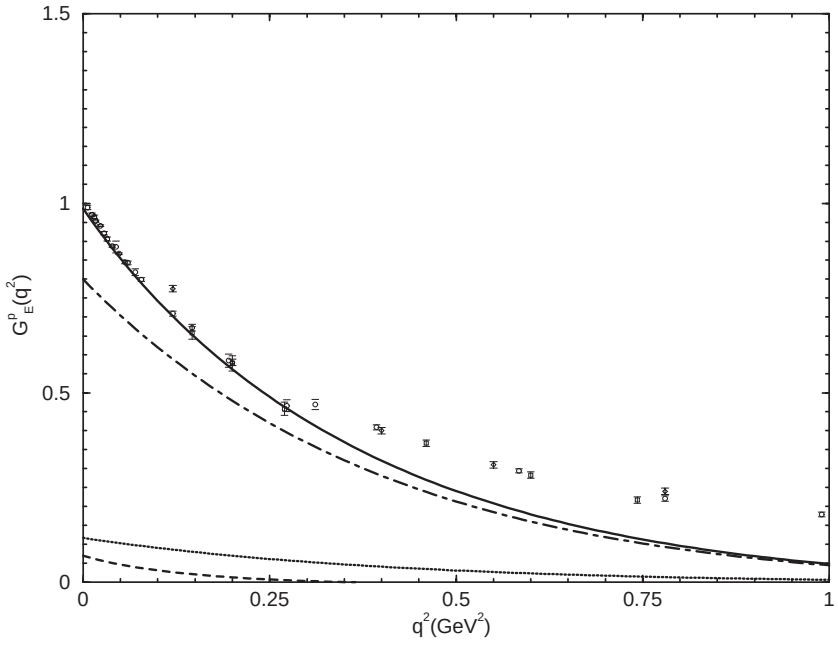

Fig. 1. The electric form factor of the proton. The dot-dashed, the dotted, the dashed and the solid curves are the contributions of Figs. 5a, 5b, 5c and the total result after renormalization. The experimental points are from [25] (circles), [26] (squares) and [27] (diamonds), respectively

electromagnetic form factors. In our calculations, we favor therefore a vanishing (or smaller) quark mass. Then, the nucleon rest mass is determined by the contributions from the confinement and the kinetic energy. This description also differs from the nonrelativistic constituent quark model, because in that model, the largest part of the nucleon mass originates from the effective constituent quark mass and the nucleon is regarded as a loosely bound state. The difference for the origin of the nucleon mass in the two approaches leads also to other distinction between the relativistic and the nonrelativistic models.

The proton electromagnetic form factors shown in Figs. 1 and 2 (for $m_q = 0$) are based on our relativistic quark model including a pion cloud. We describe nicely the proton electric and magnetic form factors without introducing any additional phenomenological mechanisms. In the nonrelativistic constituent quark model, since the harmonic oscillator length b is around b=0.5fm, the calculated root mean square radius of the charge distribution of the proton is smaller than the experiment data $\sqrt{< r^2_{Ep} >} = 0.847 \pm 0.008fm$ [32]. To improve the constituent quark model, some other mechanisms are in-

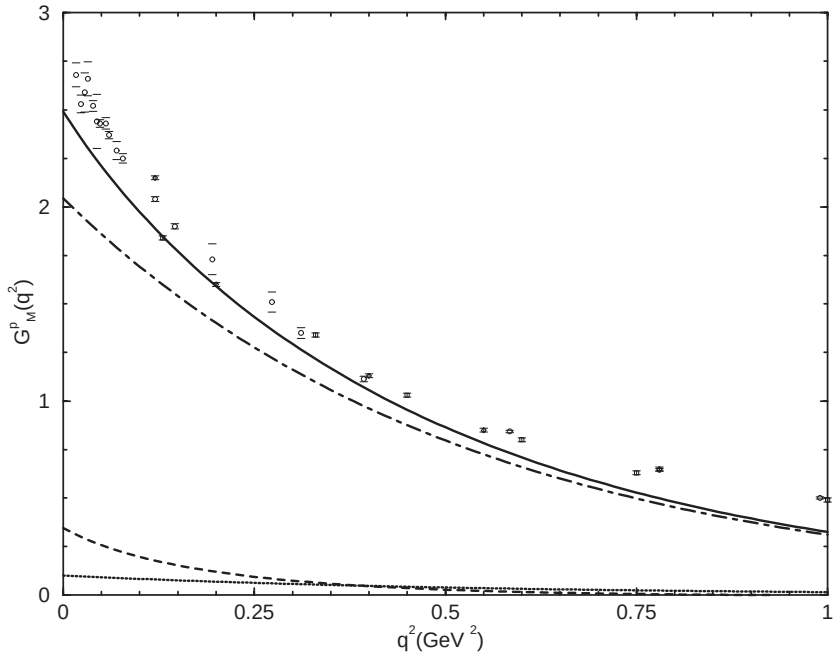

Fig. 2. The magnetic form factor of the proton. The dot-dashed, the dotted, the dashed and the solid curves are the contributions of Figs. 5a, 5b , 5c and the total result after renormalization. The experimental data are from [25] (circles), [26] (squares) and [27] (diamonds), respectively

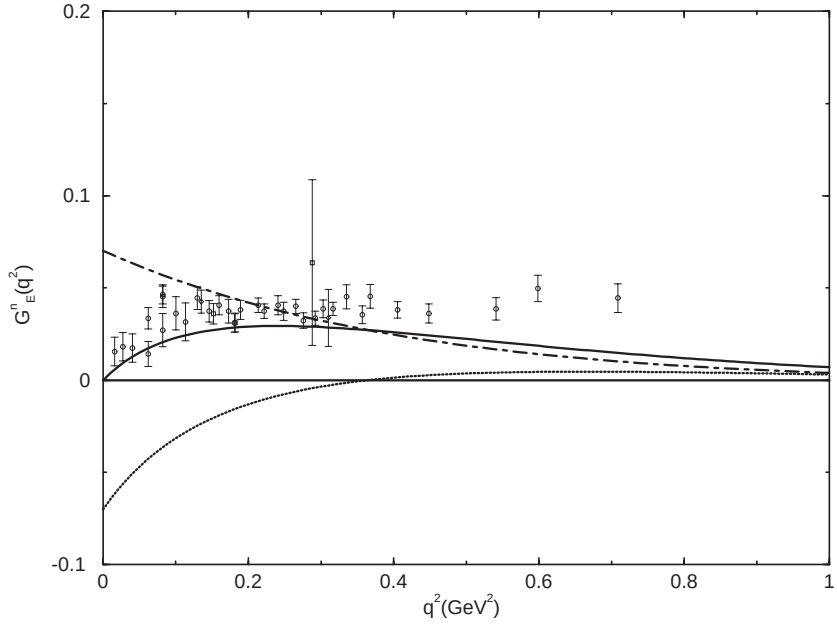

Fig. 3. The Electric form factor of the neutron. The dot-dashed, the dotted and the solid curves are the contributions of Figs. 5b, 5c and the total result after renormalization. The contribution for Fig. 5a is zero. The data are from [28] (circles) [29] (squares), and [30] (diamonds), respectively

cluded. For example, the phenomenological mono-pole form factor $F_{q\gamma}(\boldsymbol{q}^2) = 1/(1+\frac{1}{6}\boldsymbol{q}^2 r^2_{q\gamma})$ (where $r^2_{q\gamma} \simeq 6/m^2_\rho$) which simulates the electromagnetic size of the constituent quarks [33], or the contributions from the two-body exchange currents [34]. The calculation shown in table 1 indicates that our model can explain the proton root mean square charge radius reasonable well. The contributions of the diagrams shown in Figs. 5a, 5b and 5c to the observable $< r^2_{Ep} >$ are $0.469fm^2$, $0.0687fm^2$ and $0.137fm^2$ after renormalization. Consequentially, the value for the root mean square charge radius is $\sqrt{< r^2_{Ep} >} = 0.827fm$. Moreover, the contributions to the magnetic moment by the diagrams in Figs. 5a, 5b and 5c are $2.044\mu_N$, $0.101\mu_N$ and $0.346\mu_N$ (where, $\mu_N = e\hbar/2M_N c$ is nuclear magneton) after renormalization. The total value obtained for the proton magnetic moment of our model is $2.491\mu_N$, which is also in agreement with experiment $2.7928\mu_N$ [35]. We find from our calculation that in the low energy region the pion clouds play an important role for the the proton form factors. However, the pion cloud effects decrease with increasing photon three momentum $\mid \boldsymbol{q} \mid$. In addition, we also see that the magnetic moments are reduced when increasing effective quark mass. Because in the relativistic model an increase of m_q means an increase of the harmonic oscillator length (see Sect. 2) if the single

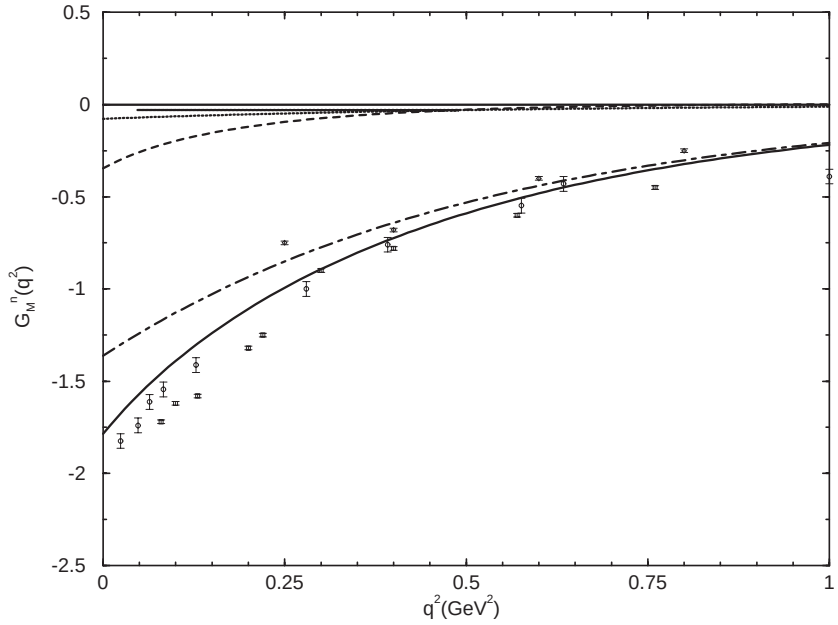

Fig. 4. The magnetic form factor of the neutron. The dotted-dashed, the dotted, the dashed and the solid curves are the contributions of Figs. 5a, 5b, 6c and the total result after renormalization. The data are from [25] (circles), [27] (squares) and [31] (diamonds), respectively

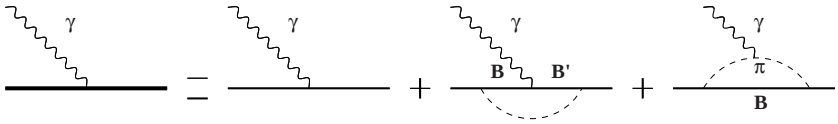

Fig. 5. Illustration of the diagrams we consider in our calculation

quark energy E_{0s} is unchanged. Thus, the relativistic calculation cannot give the same proton magnetic moment as the nonrelativistic model with the same quark mass $m_q = 350MeV$.

In our calculation for the electromagnetic form factors of the neutron, we get a nonzero value for the mean square neutron charge radius $< r_{En}^2 >$. In fact, Fig. 5a does not contribute to this physical observable as usual. Our calculation shows that the neutron charge form factor in Fig. 3 are the sum of the diagrams in Figs. 5b and 5c. This is because in the extended Fock space, the neutron wave function has an admixture of a pion-baryon contribution. The charge pion is responsible for the charge distribution of the neutron. The contribution from Fig. 5b to $< r_{En}^2 >$ is positive, whiles the contribution from Fig. 5c is negative. When $m_q = 0$ as shown in Figs. 3 and 4, the cancelation between the contributions from Fig. 5b ($< r_{En}^2 >= 0.0412fm^2$) and Fig. 5c ($< r_{En}^2 >= -0.137fm^2$) gives the total charge distribution of the neutron as shown in Fig. 3. The total mean square charge radius of the neutron is $-0.0958fm^2$ which is shown in table 1 too. This value is consistent with the data $-0.113 \pm 0.005fm^2$ [13]. Figures 3 and 4 indicate the importance of the pion cloud in the low energy region. For the magnetic moment of the neutron, the three contributions of Figs. 5a, 5b and 5c at $m_q = 0$ are $-1.362\mu_N$, $-0.0773\mu_N$ and $-0.346\mu_N$, respectively. The total calculated value for the neutron magnetic moment is therefore $-1.785\mu_N$ which is also in agreement with experimental $\mu_n = -1.9130\mu_N$[36]. Finally we found that an increase of the quark mass decreases the size of the neutron mean square radius r_{En}^2 slightly.

In conclusion we can describe well the proton and the neutron magnetic moments, the electromagnetic form factors, the charge radius of the proton and in particular of the neutron. Our results are consistent with the cloudy bag model [11] and other interpretation of the neutron charge distribution with the pion in the literature [34]. We have only two free parameters in our calculation: the quark mass and the eigenvalue of the single quark Dirac (2) E_{0s}. Our results show difference between the relativistic and the nonrelativistic approaches, because the usual parameters selected by the nonrelativistic constituent quark model are not applicable to our relativistic frame work. Moreover, we confirm the important contributions of the pion cloud for the mean square charge radius of the neutron. The pion could manifests itself especially in observables for low energies. The successful descriptions of proton and neutron properties and of the electromagnetic transitions to the $\Delta(1232)$ [12] resonance suggests that further investigations for the nucleon spin structure, for transitions of other resonances with the relativistic model are worthwhile.

Two of the authors (YBD and KS) would like to thank the Institute for Theoretical Physics, University of Tuebingen for their hospitality. This work was supported by the Alexander von Humboldt Foundation and the DAAD.

References

1. N. Isgur and G. Karl, Phys. Rev. D18 (1978), 4187; D19 (1979), 2653
2. G. Karl, Int. J. Mod. Phys. E1 (1992), 491
3. F. E. Close and Z. P. Li, Phys. Rev. D42 (1990), 2194; Z. P. Li and F. E. Close, Phys. Rev. D42 (1990), 2207; S. Capstick, Phys. Rev. D46 (1992), 1965; D46 (1992), 2864; M. Warns, H. Schroeder, W. Pfeil, and H. Rollnik, Z. Phys. C45 (1990), 627
4. Z. Dziembowski, Phys. Rev. D37 (1988), 778; H. J. Weber, Phys. Rev. D49 (1994), 3160; S. Capstick B. D. Keister, Phys. Rev. D51 (1995), 3598; F. Cardarelli, E. Pace, G. Salme and S. Simula, Phys. Lett. B397 (1997), 13; F. Cano and P. Gonzalez, Phys. Lett. B431 (1998), 270; M. De Sanctis, E. Santopinto and M. M. Giannini, Eur. Phys. J. A1 (1998), 187
5. A. De Rujula, H. Georgi, and S. L. Glashow, Phys. Rev. D12 (1975), 147
6. A. Faessler, F. Fernandez, G. Luebeck, and K. Shimizu, Phys. Lett. B112 (1982), 201; U. Straub, Z. Y. Zhang, K. Braeuer, A. Faessler S. B. Khadkikar, and G. Luebeck, Nucl. Phys. A508 (1983), 335c; A. Valcarsce, A. Faessler and F. Fernandez, Phys. Lett. B345 (1995), 367
7. G. E. Brown and M. Rho, Phys. Lett. B82 (1979), 177; R. L. Jaffe, Erice Summer School, Majorana E, Lecture, Erice 1979; A. Manohar and H. Georgi, Nucl. Phys. B234 (1984), 189; T. P. Cheng and L. F. Li, Phys. Rev. Lett. 74 (1995), 2872; E. J. Eichten, I. Hinchliffe and C. Quigg, Phys. Rev. D45 (1992), 2269; See also J. D. Bjorken, Report No. SLAC-PUB-5608 (1991) (unpublished)
8. S. Theberge, A. W. Thomas and G. A. Miller, Phys. Rev. D22 (1980), 2839; D23 (1981), 2106; A. W. Thomas, S. Theberge and G. A. Miller, Phys. Rev. D24 (1981), 216; S. Theberge, A. W. Thomas and G. A. Miller, Can. J. Phys. 60 (1982), 59; G. A. Miller, A. W. Thomas and S. Theberge, Comm. Nucl. Part. Phys. 10 (1981), 101; A. W. Thomas, Adv. in Nucl. Phys. 13 (1984), 1
9. G. Kälbermann and J. M. Eisenberg, Phys. Rev. D28 (1983), 71; K. Bermuth, D. Drechsel, L. Tiator and J. B. Seaborn, Phys. Rev. D37 (1988), 89
10. S. E. Kuhn, et al., "The polarized structure function g_1^n and the Q^2 dependence of the Gerasimov-Drell-Hearn sum rule for the neutron, CEBAF proposal No. 94-009; J. Ahrens, Mainz Proposal, 12/2-93, 1993; J. Ahrens et al., A2 Annual Report of 1996, Mainz; G. Anton et al., ELSA proposal 1992; D. Babusci et al., LEGS expt. L18/L19, 1994; L. M. Stuart et al., Phys. Rev. D58 (1998), 32003; K. A. Aniol et al., The HAPPEX Collaboration, "Measurement of the Neutral Weak Form Factors of the Proton", Submitted to Phys. Rev. Lett; V. D. Burkert, Nucl. Phys. A623 (1997), 59c; D. Dreschel, "Form Factor and Exclusive Processes Introduction and Overview', MKPH-T-98-20
11. D. H. Lu, A. W. Thomas and A. G. Williams, Phys. Rev. C57 (1998), 2628
12. Y. B. Dong, K. Shimizu, Amand Faessler and A. J. Buchmann, "Meson cloud and electroproduction of the $\Delta(1232)$ resonance in a relativistic quark model", submitted to Phys. Lett. B; Y. B. Dong, K. Shimizu, Amand Faessler and A. J. Buchmann, "Description of the electroproduction amplitudes of the Roper resonance in a relativistic quark model", Accepted by Phys. Rev. C
13. S. Kopecki et al., Phys. Rev. Lett 74 (1995), 2427
14. N. Isgur, "Interpreting the Neutron's Electric Form Factor: Rest frame Charge Distribution of Foldy Term?", JLAB-THY-98-48
15. R. E. Peierls and J. Yoccoz, Proc Phys. Soc. 70 (1957), 381; R. Tegen and R. Brockmann and W. Weise, Z. Phys. A307 (1982), 339
16. S. J. Brodsky and J. R. Primack, Ann. Phys. 52 (1969), 315
17. L. Wilets, "Non-Topological Solitons", (World Scientific, Singapore 1989); M. C. Birse, Prog. in Part. and Nucl. Phys. 25 (1990), 1
18. R. E. Peierls and D. J. Thouless, Nucl. Phys. 38 (1962), 154; D. H. Lu, A. W. Thomas and A. G. Williams, Phys. Rev. C55 (1997), 3108
19. K. Shimizu, Y. B. Dong, A. Faessler, A. J. Buchmann, "Relativistic treatment of constituent quark model", Submitted to Nucl. Phys. A
20. M. Gell-Mann, R. J. Oakes and B. Renner, Phys. Rev. 175 (168), 2195; J. Gasser and H. Leutwyler, Phys. Rept. 87 (1982), 77
21. T. Ericson and W. Weise, "Pion and Nuclei", (Oxford Science Publications, 1988)
22. N. Barik and B. K. Dash, Phys. Rev. D33 (1986), 1925; Phys. Rev. D34 (1986); 2092; N. Barik, S. N. Jena, D. P. Rath, Phys. Rev. D41 (1990), 1568
23. S. Theberge and A. W. Thomas, Nucl. Phys. A393 (1983), 252
24. A. W. Thomas and G. Krein, "Chiral corrections in hadron spectroscopy", Nucl-th/9902013
25. G. Höhler et al., Nucl. Phys. B114 (1976), 505
26. R. C. Walker et al., Phys. Rev. D49 (1994), 5671
27. W. Bartel et al., Nucl. Phys. B58 (1973), 429
28. S. Platchkov, et al., Nucl. Phys. A510 (1990), 740
29. T. Eden et al., Phys. Rev. C50 (1994), 1749
30. M. Meyerhoff et al., Phys. Lett B327 (1994), 201
31. K. M. Hanson et al., Phys. Rev. D8 (1973), 753
32. D. Drechsel et al., "Hadron polarizabilities and form factors", Nucl-th/9712013
33. U. Vogl and W. Weise, Prog. Part. Nucl. Phys. 27 (1991), 195; V. A. Petrunkin, Sov. J. Part. Nucl. 12 (1981), 278; D. P. Stanley and D. Robson, Phys. Rev. D26 (1982), 223
34. A. J. Buchmann, H. Hernandez and K. Yazaki, Phys. Lett B269 (1991), 25, A. J. Buchmann, H. Hernandez and Amand Faessler, Phys. Rev. C55 (1997), 448; A. J. Buchmann, H. Hernandez, U. Meyer and Amand Faessler, Phys. Rec. C58 (1998), 2478
35. Particle Data Group, Phys. Lett. B170 (1986), 11
36. S. D. Drell and F. Zachariasen, "Elecrtomagnetic Structure of Nucleons", (Oxford University press, New York, 1961); R. Hofstadter, "Nucleon and Nucleon Structure" (W. A. Benjamin, Inc., 1963); L. Hand, D. G. Miller and R. Wilson, Rev. Mod. Phys. 35 (1963), 335